Integrity of the network sarcoplasmic reticulum in skeletal muscle requires small ankyrin 1

Maegen A. Ackermann[1], Andrew P. Ziman[2], John Strong[2,*], Yinghua Zhang[2], April K. Hartford[2,‡], Christopher W. Ward[3], William R. Randall[4], Aikaterini Kontrogianni-Konstantopoulos[1] and Robert J. Bloch[2,§]

[1]Department of Biochemistry and Molecular Biology, [2]Department of Physiology, [3]School of Medicine and School of Nursing, and [4]Department of Pharmacology and Experimental Therapeutics University of Maryland, Baltimore, MD 21201, USA

*Present address: School of Dentistry, University of Maryland, Baltimore, MD 21201, USA
‡Present address: Community College of Baltimore County, Baltimore, MD 21237, USA
§Corresponding author (rbloch@umaryland.edu)

Accepted 6 June 2011
Journal of Cell Science 124, 3619–3630

doi: 10.1242/jcs.085159

Summary

Small ankyrin 1 (sAnk1; Ank1.5) is a ~20 kDa protein of striated muscle that concentrates in the network compartment of the sarcoplasmic reticulum (nSR). We used siRNA targeted to sAnk1 to assess its role in organizing the sarcoplasmic reticulum (SR) of skeletal myofibers in vitro. siRNA reduced sAnk1 mRNA and protein levels and disrupted the organization of the remaining sAnk1. Sarcomeric proteins were unchanged, but two other proteins of the nSR, SERCA and sarcolipin, decreased significantly in amount and segregated into distinct structures containing sarcolipin and sAnk1, and SERCA, respectively. Exogenous sAnk1 restored SERCA to its normal distribution. Ryanodine receptors and calsequestrin in the junctional SR, and L-type Ca^{2+} channels in the transverse tubules were not reduced, although their striated organization was mildly altered. Consistent with the loss of SERCA, uptake and release of Ca^{2+} were significantly inhibited. Our results show that sAnk1 stabilizes the nSR and that its absence causes the nSR to fragment into distinct membrane compartments.

Key words: Sarcoplasmic reticulum, Skeletal muscle, Ankyrin

Introduction

The function of skeletal muscle requires the integration of the sarcomere, the sarcoplasmic reticulum (SR) and the transverse tubules. These components are functionally linked during excitation–contraction (EC) coupling, in which an action potential depolarizes the transverse (t-)tubules, which are specialized branches of the sarcolemma. This depolarization causes a conformational change in the L-type Ca^{2+} channels (dihydropyridine receptors, DHPRs), which are found primarily in the t-tubules. Opening of the DHPRs triggers the release of Ca^{2+} from the SR, the primary Ca^{2+}-storage organelle within the fiber, through SR Ca^{2+} channels (ryanodine receptors, RyRs) (Schneider and Chandler, 1973). The rapid increase in cytosolic [Ca^{2+}] causes a cascade of molecular events resulting in contraction of the sarcomeres. Relaxation occurs when cytosolic [Ca^{2+}] is reduced to resting levels as the SR-ER Ca^{2+}-ATPase (SERCA) refills the SR Ca^{2+} stores.

The SR is organized into at least two distinct functional domains, the junctional SR (jSR) and the network SR (nSR), which together envelope the contractile apparatus. In mammalian skeletal muscle, the jSR (or terminal cisternae) is found at the overlap of the A- and I- bands (A–I junction) of the sarcomere, closely apposed to the t-tubules, and is the primary site for storage and release of Ca^{2+} in striated muscle. The jSR membrane contains RyRs, which are physically coupled to the DHPRs of the t-tubules. The lumen of the jSR contains proteins (e.g. triadin, junctin and calsequestrin) that modulate the activity of the RyR by regulating the buffering of Ca^{2+} (Gyorke et al., 2004). The nSR is a system of tubules that wrap around the sarcomere, specifically around the M-band and Z-disk, and are connected to nearby jSR (Franzini-Armstrong et al., 2005). Most of the SERCA in skeletal muscle is in the nSR (Jorgensen et al., 1982), which therefore has a key role in Ca^{2+} homeostasis. The efficacy of EC coupling in mature skeletal muscle is dependent upon the periodic organization of the SR and t-tubules around the sarcomere, which in turn requires anchoring mechanisms that are strong enough to resist the stresses associated with the contractile cycle. Here we explore the role of a small form of ankyrin (sAnk1) in organizing the nSR around the Z-disks and M-bands of skeletal myofibers in culture.

Small ankyrin 1 (sAnk1, Ank1.5) (Bagnato et al., 2003; Birkenmeier et al., 1998), a small (~20 kDa) protein of striated muscle (Zhou et al., 1997), is a product of the *ANK1* gene and shares homology with larger members of the ankyrin superfamily (Birkenmeier et al., 1998; Borzok et al., 2007). Ankyrins are ubiquitously expressed proteins that typically function to link integral membrane proteins to cytoskeletal components. sAnk1 is one of the first SR proteins to become organized during the development of skeletal muscle (Giacomello and Sorrentino, 2009). It localizes to membranes around M-bands and Z-disks but not at the A–I junction (Zhou et al., 1997), indicating that it concentrates in the nSR. The N-terminal hydrophobic 29 amino acid sequence of sAnk1 is sufficient to anchor and target the protein to the nSR (Porter et al., 2005). The C-terminal cytoplasmic portion of sAnk1 binds specifically and with high affinity to the C-terminal region of obscurin, located at the

periphery of both M-bands and Z-disks (Bagnato et al., 2003; Kontrogianni-Konstantopoulos and Bloch, 2005; Kontrogianni-Konstantopoulos et al., 2003), and with lower affinity to the two most N-terminal Ig domains of titin, located at Z-disks (Kontrogianni-Konstantopoulos and Bloch, 2003).

Although it binds to obscurin and titin, two of the largest proteins of striated muscle (Kontrogianni-Konstantopoulos et al., 2009), the role of sAnk1 is still unclear. Reduced expression of obscurin, induced by a targeted small interfering RNA (siRNA), results in the disorganization of sAnk1 and possibly of the nSR (Kontrogianni-Konstantopoulos et al., 2006b). Similarly, elimination of obscurin by homologous recombination alters the stability of both sAnk1 and the nSR (Lange et al., 2009). These data support the idea that sAnk1 forms a link between the nSR and the contractile apparatus through its interaction with obscurin and titin at M-bands and Z-disks. However, they do not indicate whether sAnk1 is either necessary or sufficient for anchoring the nSR to contractile structures, or indeed whether it has additional roles in the stability of this membrane compartment. Here, we use siRNA targeted to sAnk1 (sAnk1-siRNA) to test its role in the organization and function of the SR in adult myofibers. Our results suggest a role for sAnk1 in maintaining the integrity of the nSR and its organization around the contractile apparatus.

Results

Targeted siRNA reduces sAnk1 expression and alters its localization

We used RNAi technology to inhibit the synthesis of sAnk1 in primary cultures of rat flexor digitorum brevis (FDB) myofibers and then studied the effects on the stability of the SR. We prepared adenovirus expressing siRNA targeted to a sequence in the 5′ UTR of sAnk1, present in the region of the *Ank1* gene that encodes small muscle-specific isoforms, ~150 nucleotides upstream of its start codon (sAnk1-siRNA). Database searches showed that the targeted sequence is specific for the small muscle specific transcripts of the *Ank1* gene (sAnk1/Ank1.5, Ank1.6 and Ank1.9). Ank1.6 and Ank1.9 are not present in murine FDB muscle (see below and supplementary material Fig. S1) and are therefore not a concern for this study. Myofibers infected with virus expressing an irrelevant siRNA (con-siRNA) served as controls. We infected FDB fibers with adenovirus encoding sAnk1-siRNA or con-siRNA 24 hours after initial plating and assayed the effects of viral transduction 48 hours later.

Western blots showed a 59±3.2% reduction in the amount of the ~20 kDa form of sAnk1 expressed in myofibers transduced with sAnk1-siRNA, compared with controls ($P<0.01$; Fig. 1A,C). RT-PCR with primers to the 5′ and 3′ coding regions of sAnk1 showed that the levels of the transcript were reduced by 63±2.9% ($P<0.01$; Fig. 1B,C). RT-PCR of extracts of myofibers treated with either con-siRNA or sAnk1 failed to detect mRNA encoding other small variants of Ank1 (specifically Ank1.6 and Ank1.9; supplementary material Fig. S1A).

Immunofluorescence studies with an antibody specific for sAnk1 (Zhou et al., 1997) revealed that sAnk1 in untransduced FDB fibers or in fibers transduced with con-siRNA localized primarily at the Z-disk, with smaller amounts at the M-band (Fig. 1D1, Z-disk indicated by arrow), as previously reported (Zhou et al., 1997). Fluorescence profiles of regions of interest (ROIs) confirmed this striated pattern, with larger and smaller peaks representing the staining of Z-disks and M-bands, respectively. In cultures transduced with virus expressing sAnk1-siRNA, ~80% of the fibers showed reduced labeling for sAnk1 (Fig. 1D, 2 and 3). The normalized fluorescent intensity of the sAnk1 label in 'knockdown' (KD) fibers, decreased by 58±3.4% over the entire population ($P<0.01$; Fig. 1C), which correlates well with the amount of protein lost. However, the extent to which sAnk1 was reduced varied among fibers.

When we categorized the severity of sAnk1 knockdown, we found that ~15% of the fibers showed little or no detectable sAnk1 (Fig. 1D3), without distinct peaks at Z-disks or M-bands, whereas ~65% still showed distinct, albeit dimmer and more punctate, labeling that concentrated near Z-disks (Fig. 1D2). The latter group also displayed longitudinal elements. We categorized these as severely and moderately affected, respectively. Quantification of the disruption of sAnk1 (supplementary material Fig. S2) showed that the variances of peak-to-peak

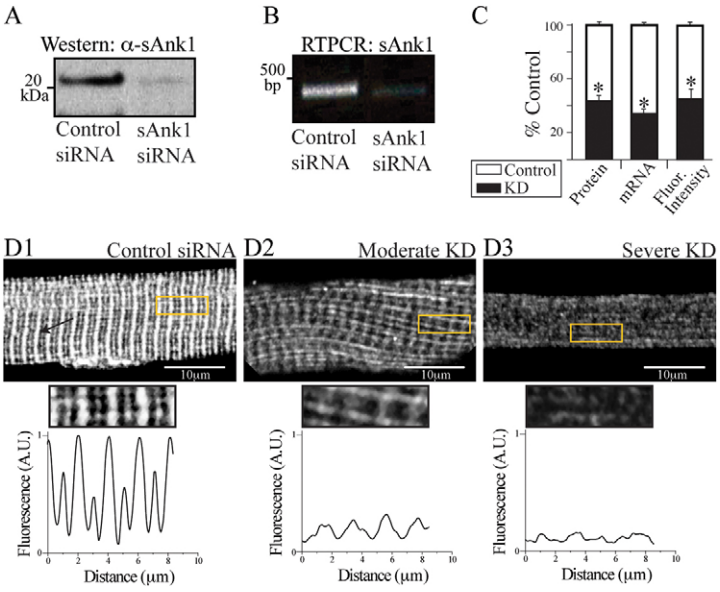

Fig. 1. Effect of targeted siRNA on sAnk1 mRNA and protein levels. FDB fibers were transduced with adenovirus encoding siRNA selective for sAnk1 or a control sequence. Samples were maintained in culture for 48 hours and then examined by western blotting, RT-PCR and immunofluorescence. (**A**,**B**) sAnk1 protein (A) and mRNA (B) are reduced in cultures of fibers treated with sAnk1-siRNA. (**C**) Mean sAnk1 protein, cDNA and fluorescent intensity levels are significantly reduced (>50%) in cells treated with sAnk1-siRNA (KD), compared with controls (*$P<0.01$, Student's *t*-test). Results are means ± s.e.m. (**D**) In con-siRNA-treated myofibers (D1), sAnk1 concentrates around Z-disks, and to a lesser extent around M-bands, as indicated by the regular fluorescent peaks. Myofibers treated with sAnk1-siRNA (D2, D3), show a range of intensities and distribution, from little (similar to controls; not shown), to moderate (D2) and severe (D3); 5× regions of interest (ROIs) boxed in yellow. Severely affected fibers (D3) constitute ~15% of the total. Most fibers are only moderately affected (D2), and show reduced labeling for sAnk1, that is absent around the M-band, and present in some longitudinal structures. The arrow in D1 indicates Z-disks. See also supplementary material Fig. S1. The results show that sAnk1-siRNA reduces sAnk1 levels and alters its distribution in skeletal myofibers.

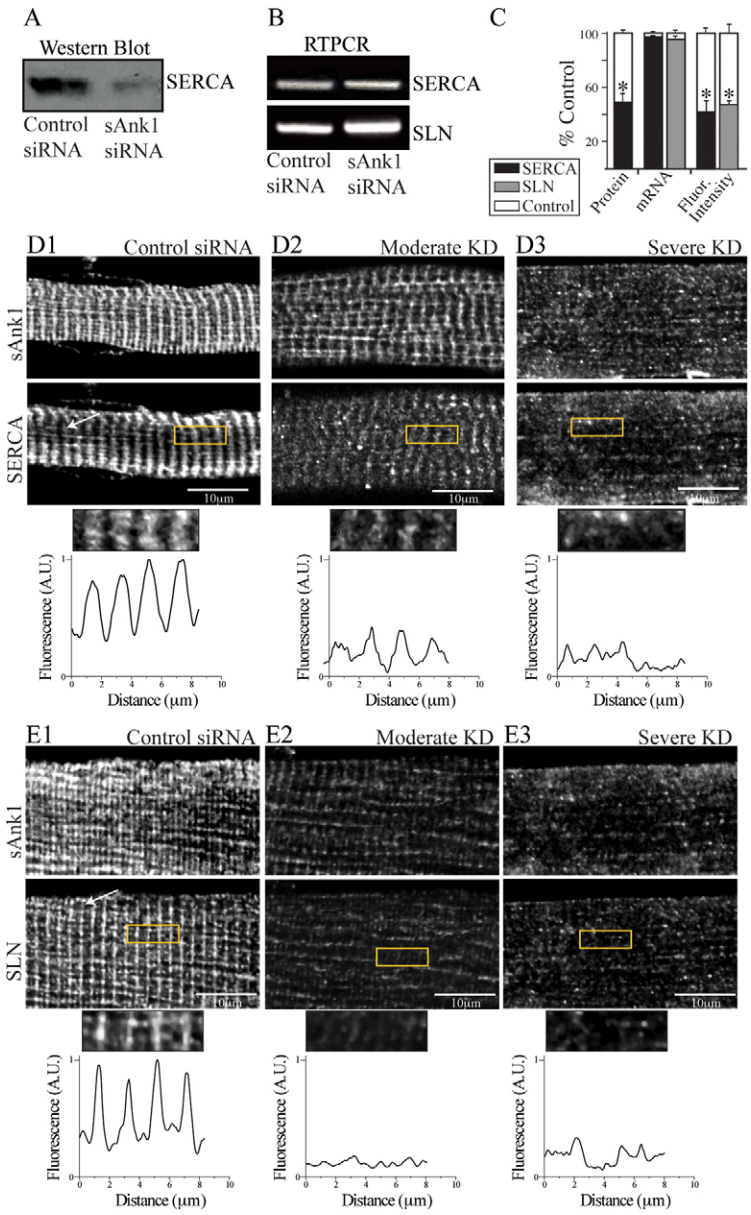

Fig. 2. Reduced expression of sAnk1 leads to disruption of the network SR. FDB myofibers were treated as in Fig. 1 and analyzed for two components of the nSR, SERCA and SLN. (**A**) SERCA protein is significantly reduced in immunoblots of myofibers treated with sAnk1-siRNA, compared with con-siRNA. (**B**) Levels of mRNA encoding SERCA and SLN are not altered in myofibers in which sAnk1 expression is reduced. (**C**) Intensity of immunofluorescence labeling of SERCA and SLN are both significantly reduced (>50%) in cells treated with sAnk1-siRNA, compared with controls. Results are means ± s.e.m. (**D**,**E**) The organization of SERCA (D2,D3) and SLN (E2,E3), is disrupted or lost when sAnk1 expression is inhibited as compared with controls (D1 and E1, respectively). Fluorescent profiles of the ROI (yellow boxes) illustrate the normal, striated pattern of SERCA and SLN, which localize primarily at the Z-disks in control fibers (bottom left panels of D1 and E1, respectively), which is lost in fibers with very low levels of sAnk1 (bottom right panels of D3 and E3, respectively). The results show that sAnk1-siRNA reduces the amount of SERCA and SLN proteins, but not their mRNAs, and alters their distribution in skeletal myofibers.

distances between control and experimental fibers for both moderately and severely affected fibers were significantly different from controls ($P<0.01$; Fig. 6A, black dots). These results suggest that the reduced expression of sAnk1 by targeted siRNA causes not only a loss of the sAnk1 protein, but also a disruption of its organization.

We used antibodies against ankyrin B and ankyrin G in immunofluorescence experiments to learn whether, similarly to sAnk1, their levels of expression and localization were altered by siRNA treatment. The fluorescence intensity and pattern of ankyrin B, which concentrates at the M-bands and Z-disks of skeletal muscle (Mohler, 2006), and of ankyrin G, which concentrates mainly at the sarcolemma with faint staining at the SR (Hopitzan et al., 2005; Kordeli et al., 1998), were not altered in myofibers transduced with siRNA targeted to sAnk1 (supplementary material Fig. S1B,C). These results are consistent with the specificity of the siRNA we used for the ~20 kDa form of sAnk1 and suggest that other muscle-specific ankyrins are not affected by the loss of sAnk1.

Effects on proteins of the network SR

Similarly to sAnk1, SERCA and sarcolipin (SLN) concentrate at the Z-disks and M-bands, and are components of the nSR (Franzini-Armstrong et al., 1986; Odermatt et al., 1998). sAnk1-siRNA had no effect on the level of mRNAs encoding these proteins (Fig. 2B,C), but the amount of SERCA protein in siRNA-treated myofibers decreased by 55±4.2%, compared with controls ($P<0.01$; Fig. 2A,C). Consistent with this, as well as our results for sAnk1, immunofluorescence studies of SERCA in treated myofibers showed an overall reduction of 60±13% compared with controls ($P<0.01$). In fibers in which sAnk1 was severely reduced, SERCA, like sAnk1, was only detectable in small punctate structures (Fig. 2D3; see below). Fluorescent profiles of these images showed no distinguishable peaks

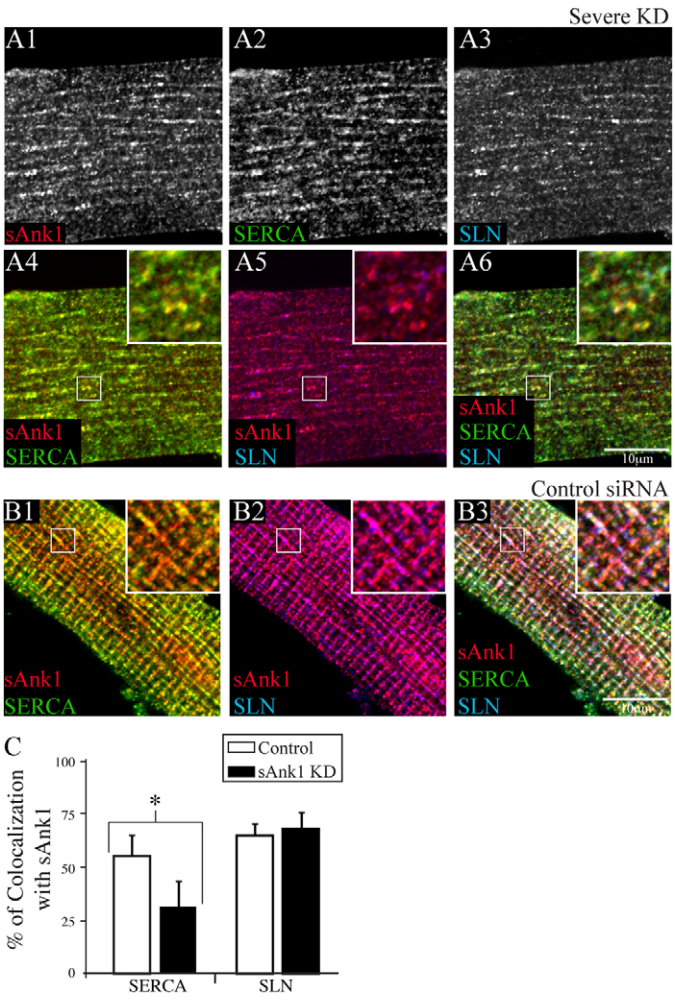

Fig. 3. Residual proteins of the nSR appear in punctate or longitudinal structures when sAnk1 is severely reduced. Myofibers treated as in Fig. 1 were triple labeled for immunofluorescence of sAnk1, SERCA and SLN. (**A**) Fibers with severely reduced expression of sAnk1 show remaining sAnk1 (A1), SERCA (A2) and SLN (A3) in punctate or longitudinal structures. SERCA and SLN are compared with sAnk1 in color overlays (A4, sAnk1 and SERCA in yellow; A5, sAnk1 and SLN in purple; A6, all three, in white). (**B**) In control fibers, all proteins colocalize at the Z-disk (sAnk1, red; SERCA, green; and SLN, blue; other colors are as above). (**C**) Colocalization of each protein with sAnk1 was determined by Pearson's correlation coefficient. In fibers treated with sAnk1-siRNA, the colocalization of SERCA and sAnk1 is significantly reduced (*$P<0.01$), but colocalization of SLN and sAnk1 is unchanged. The results show that the components of the nSR segregate into distinct structures when sAnk1 is reduced. Data are means ± s.e.m.

corresponding to Z-disks or M-bands. Myofibers with a moderate disruption of sAnk1 had moderate reductions in SERCA, which like sAnk1 concentrated primarily around Z-disks, albeit at reduced amounts (Fig. 2D2).

We could not assay the amount of SLN protein in western blots, but immunofluorescence studies showed that its expression was also greatly reduced (55±3.8%, compared with controls; $P<0.01$; Fig. 2C) and its distribution was severely disorganized in myofibers that had low levels of sAnk1 after siRNA treatment (Fig. 2E3), which is similar to the effects on SERCA and sAnk1. Similarly to SERCA, SLN in myofibers showing only moderate reduction in sAnk1 levels concentrated with sAnk1 at the level of Z-disks (Fig. 2E2), whereas labeling in fibers expressing very low levels of sAnk1 was disorganized and punctate.

We quantified the disruption of SERCA and SLN that remained in myofibers following the knockdown of sAnk1 by siRNA. The variances of peak-to-peak distances between control and experimental fibers resembled those of sAnk1 and were significantly different from controls in moderately and severely affected fibers for both SERCA and SLN ($P<0.01$; Fig. 6A, light and dark grey, respectively). These results suggest that proteins of the nSR are disrupted when the expression of sAnk1 is inhibited.

We compared the distributions of SERCA and SLN with that of sAnk1 in myofibers that showed extensive loss of all three proteins. Most of the small, punctate structures that labeled for SLN also labeled for sAnk1, whereas those containing SERCA tended to be distinct (Fig. 3). Calculation of Pearson's coefficient showed 69±8.4% colocalization of sAnk1 and SLN in this population of fibers, which is similar to the amount of colocalization seen in controls (66±6.0%; $P>0.05$; Fig. 3C). By contrast, colocalization of sAnk1 and SERCA in these myofibers decreased from 57±10% in controls to 32±12% ($P<0.01$). These results suggest that, when the nSR is destabilized by sAnk1-siRNA, two populations of punctate structures appear, one of which is enriched in both sAnk1 and SLN, and the other in SERCA.

Proteins of the triad junction and sarcomere

We examined proteins of the triad junction to learn whether their expression and organization was affected by sAnk1-siRNA. PCR experiments showed no significant changes in mRNA for calsequestrin, compared with controls (Fig. 4B), and immunoblots of RyR and calsequestrin showed no loss of either protein in siRNA-treated cultures (Fig. 4A,C). Immunofluorescence studies revealed that the normally crisp doublet labeling at the A–I junction, characteristic of RyR and calsequestrin, seen in control myofibers (Fig. 4D1,E1, respectively), became marginally more punctate, with distinct longitudinal components appearing in some myofibers with a moderate reduction in sAnk1 (Fig. 4D2,E2, respectively). In

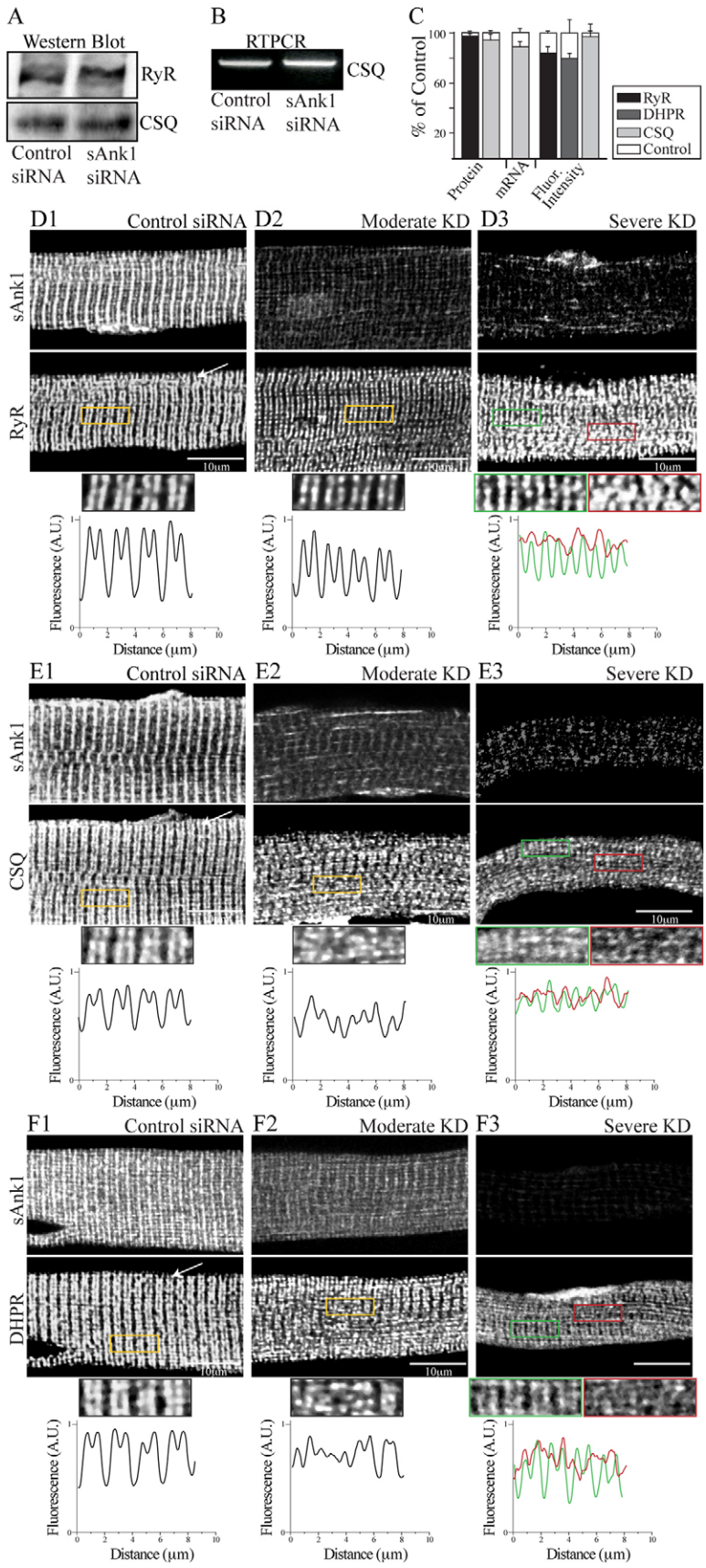

Fig. 4. Proteins of the triad junction are mildly altered when sAnk1 is severely reduced. Myofibers were treated as in Fig. 1. Extracts were prepared and analyzed for protein and mRNA levels, or for the distribution of proteins of the jSR (RyR; DHPR; calsequestrin, CSQ). (**A**) RyR and CSQ polypeptides are unaffected by sAnk1-siRNA. (**B**) mRNA encoding CSQ is unchanged. (**C**) Mean protein and mRNA expression and fluorescent intensity levels do not significantly change when sAnk1 is reduced ($P<0.01$, Student's *t*-test). Results are means ± s.e.m. (**D**–**F**) Fluorescent profiles of the boxed ROIs show the normal doublet pattern for RyR, CSQ and DHPR at the A–I junction of control myofibers (bottom panels D1, E1 and F1, respectively) in control fibers. When sAnk1 is moderately reduced, this doublet is disrupted in some regions but stable in most. When sAnk1 is severely reduced, all three antibodies continue to label doublets over many areas of the myoplasm (ROIs in green), but other areas are partially disrupted (ROIs in red). The results show that proteins of the triad junction undergo a small to moderate change in organization when sAnk1 expression is inhibited.

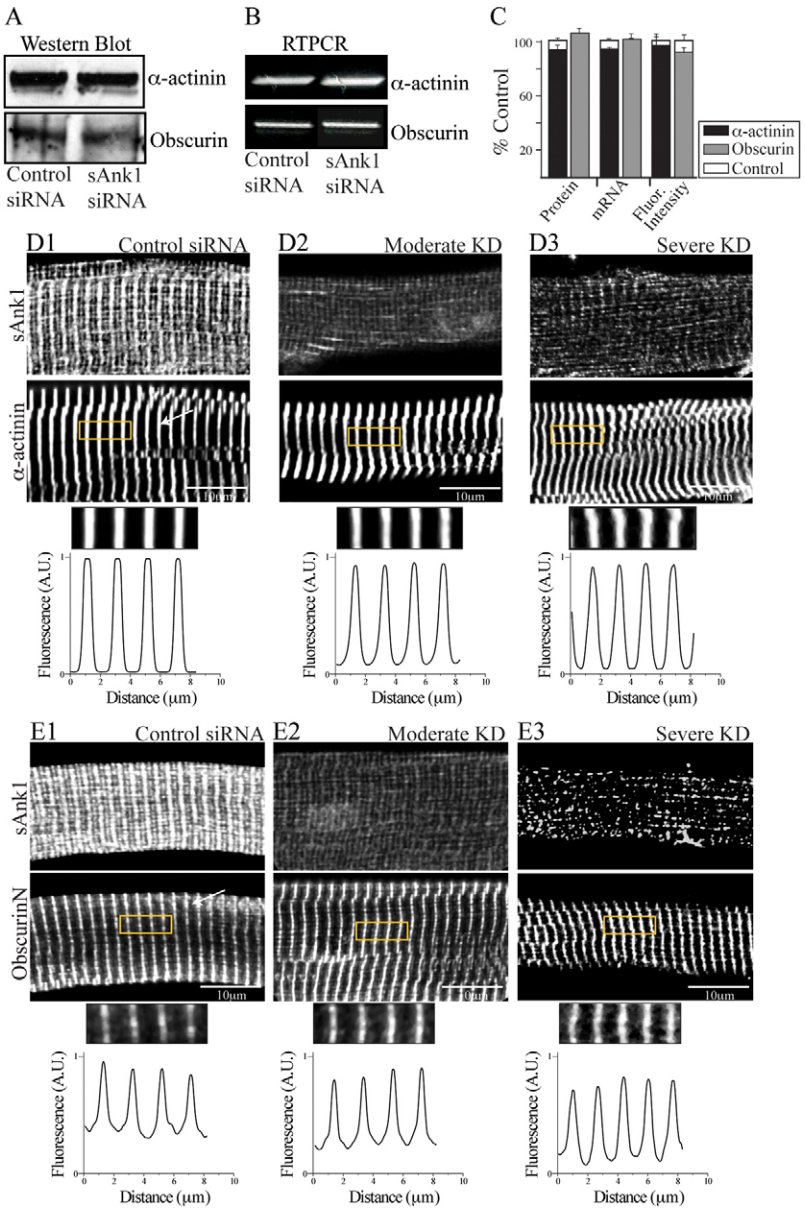

Fig. 5. Sarcomeric proteins are unaffected when sAnk1 is reduced. Myofibers were treated as in Fig. 1 and examined for expression of α-actinin and obscurin. (**A**) Immunoblot of α-actinin and obscurin indicate that these proteins are unchanged when sAnk1 expression is reduced. (**B**) RT-PCR shows that the mRNAs encoding α-actinin and obscurin are also unaffected. (**C**) Quantitative comparisons of the amounts of α-actinin and obscurin and their mRNAs, as well as the intensity of immunofluorescence labeling, reveal no significant differences between controls and myofibers treated to reduce expression of sAnk1 ($P<0.01$ Student's *t*-test). Results are means ± s.e.m. (**D**,**E**) Immunofluorescence labeling for α-actinin (D) and obscurin (E) reveals no significant differences in the organization of these two proteins in myofibers with either moderately or severely reduced expression of sAnk1. The antibody against obscurin recognizes the N-terminal Ig domains and labels only M-bands. α-Actinin is limited to Z-disks. The results show that the contractile apparatus is not significantly affected by sAnk1-siRNA.

fibers with more severe knockdown of sAnk1, proteins of the triad junction appeared as punctate doublets at the A–I junction, with poorer organization in limited regions (Fig. 4D3,E3, green and red boxed regions, respectively). DHPR, a protein of transverse tubules that colocalizes with RyR, gave similar results (Fig. 4F). The extent of disruption of the organization of RyR at triad junctions, quantified as described above, was only significantly affected in myofibers showing a severe knockdown in sAnk1 ($P<0.01$), whereas DHPR and calsequestrin were significantly disrupted in myofibers showing either moderate or severe loss of sAnk1 ($P<0.01$; Fig. 6B, black, light and dark grey dots, respectively). Nevertheless, the intensities of immunofluorescence staining of all three proteins were indistinguishable from controls (Fig. 4C; $P>0.05$). These results suggest that the jSR is less severely affected than the nSR when the expression of sAnk1 is suppressed.

We also examined proteins associated with the contractile apparatus. α-Actinin and obscurin, the major ligand for sAnk1 (Bagnato et al., 2003; Kontrogianni-Konstantopoulos et al., 2003), studied with antibodies against the extreme N-terminus, RhoGEF domain and C-terminus of the protein, showed normal amounts of protein in immunoblots and mRNA in RT-PCR in cultures of sAnk1-siRNA-treated myofibers (Fig. 5A–C). Their average immunofluorescent intensities also did not change significantly (Fig. 5C; S3C). Neither the distribution of obscurin at M-bands or Z-disks nor that of α-actinin at Z-disks was disrupted in sAnk1-siRNA-treated fibers (Fig. 5D,E; supplementary material Fig. S3C). Both obscurin and α-actinin remained tightly organized when the expression of sAnk1 was reduced to either a moderate or severe degree (Fig. 6C, grey and black, respectively). Other sarcomeric markers localized to Z-disks (the most N-terminal portion of titin, another ligand for sAnk1), A- and M-bands (myosin and myomesin, respectively) were also unaffected in myofibers with reduced levels of sAnk1, as assessed by immunofluorescence (supplementary material Fig. S3), immunoblotting and RT-PCR (not shown). Thus, inhibition

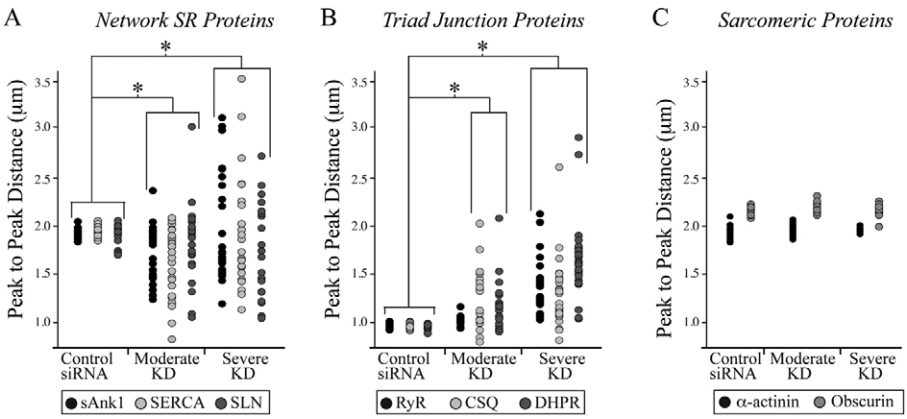

Fig. 6. Quantification of loss of organization of proteins in myofibers with reduced levels of sAnk1. The distribution of proteins in control and siRNA-treated fibers was measured by calculating the average peak-to-peak distances (see Materials and Methods, and supplementary material Fig. S2) and comparing the values seen in control myofibers with those seen in myofibers showing moderate or severe reduction in expression of sAnk1 ($n=25$ per group). (**A**) The loss of organization of three proteins of the nSR, sAnk1 (black), SERCA (light grey) and SLN (dark grey) are very similar and differ significantly from controls in populations in which sAnk1 is either moderately or severely reduced (*$P<0.01$, F-test). (**B**) Proteins of the jSR, including RyR (black), CSQ (light grey) and DHPR (dark gray) show significant peak-to-peak variation in the myofibers having severely reduced levels of sAnk, compared with controls (*$P<0.01$, F-test). DHPR and CSQ also show significant variation in myofibers with moderate reduction in sAnk1 (*$P<0.01$, F-test). (**C**) Two proteins associated with the contractile apparatus, α-actinin (black) and obscurin (grey) show no significant variation in the average peak-to-peak distances between control and affected groups ($P>0.05$, F-test).

of expression of sAnk1 with targeted siRNA has no effect on the expression or organization of proteins associated with sarcomeres.

Ultrastructural effects of sAnk1-siRNA

We also used thin-section electron microscopy to examine myofibers treated with sAnk1-siRNA or con-siRNA. Micrographs of longitudinal sections of controls showed the expected organization of sarcomeres, t-tubules and SR (Fig. 7A1, B1, C1, respectively). In particular, sarcomeres were organized in crisp striations, t-tubules and triad junctions were organized regularly at the periphery of the myofibrils, at or near the level of A–I junctions, and the nSR appeared as an anastomosing network of membrane-bound tubules centered predominantly over the Z-disk. Clear membrane profiles positioned over the A-bands or M-bands were rare. Myofibers treated with sAnk1-siRNA showed normal organization of sarcomeres and triad junctions (Fig. 7A2, B2), but the anastomosing network of nSR tubules was partially disrupted and swollen, and longitudinal elements of the SR were prominent (Fig. C2, swollen elements indicated by an asterisk), in agreement with our immunofluorescence studies.

Restoration of nSR with chimeric sAnk1

We next tested the ability of exogenous sAnk1, expressed following transfection of FDB muscles with plasmid encoding sAnk1–mCherry, to prevent the disruption of the nSR caused by sAnk1-siRNA. We used electroporation (DiFranco et al., 2006) to transfect myofibers in situ with cDNA encoding the fusion protein, which lacks the 5′UTR sequence targeted by the siRNA. A plasmid encoding mCherry alone served as control. One week later, the myofibers were cultured, treated with adenovirus encoding sAnk1-siRNA and 2 days later stained for endogenous sAnk1 and SERCA. The sAnk1–mCherry construct did not label with the sAnk1 antibody recognizing the 15 C-terminal amino acids of sAnk1 (Zhou et al., 1997) either in immunofluorescence or immunoblots, presumably because the mCherry moiety at the C-terminus of sAnk1 blocked access to the epitope (Y.Z. and R.J.B., unpublished results). Controls, expressing mCherry alone (Fig. 8A1), showed the disrupted organization of endogenous sAnk1 and SERCA (Fig. 8A2, A3), presented above. By contrast, myofibers expressing sAnk1-mCherry showed the normal pattern of labeling for SERCA in transverse structures at the level of Z-disks (Fig. 8B1), which was similar to the organization of the exogenous sAnk1–mCherry (Fig. 8B3), despite the severe depletion of the endogenous protein (Fig. 8B2). These results suggest that the effects of sAnk1-siRNA are specific for sAnk1.

Effect on SR $[Ca^{2+}]_i$ content

We measured $[Ca^{2+}]_i$ transients elicited in intact myofibers by 4-chloro-m-cresol (4-CmC), a potent agonist of the RyR, using FDB fibers loaded with the Ca^{2+} indicator, Fluo-4, and confocal line-scan imaging. Representative fluorescence profiles (Fig. 9A) show a clear difference in the response to 4-CmC between myofibers treated with sAnk1-siRNA and those treated with con-siRNA. The former had an approximately 40% reduction in the peak of the $[Ca^{2+}]_i$ transient, compared with controls (con-siRNA, 6.16 ± 0.43; sAnk1-siRNA, 3.81 ± 0.53; Fig. 9B, $P<0.01$; $n=14$ and $n=17$, respectively). We assessed the ability of SERCA to refill the SR by fitting the fluorescence profile of the rapid phase of the decay phase of the $[Ca^{2+}]_I$ transient to an exponential. The decay constant, tau, was nearly 30% (control, 8.0 ± 0.69; siRNA, 10.8 ± 0.65) larger in fibers treated with sAnk1-siRNA, compared with controls (Fig. 9C, $P<0.01$), consistent with the reduced levels of SERCA in sAnk1-siRNA-treated fibers.

Discussion

Ca^{2+} homeostasis in striated muscle is essential for EC coupling, which in turn is dependent on the proper alignment and organization of internal membranes, including the nSR, around the contractile apparatus. We have examined the role of sAnk1 in maintaining the organization of the nSR by targeting its

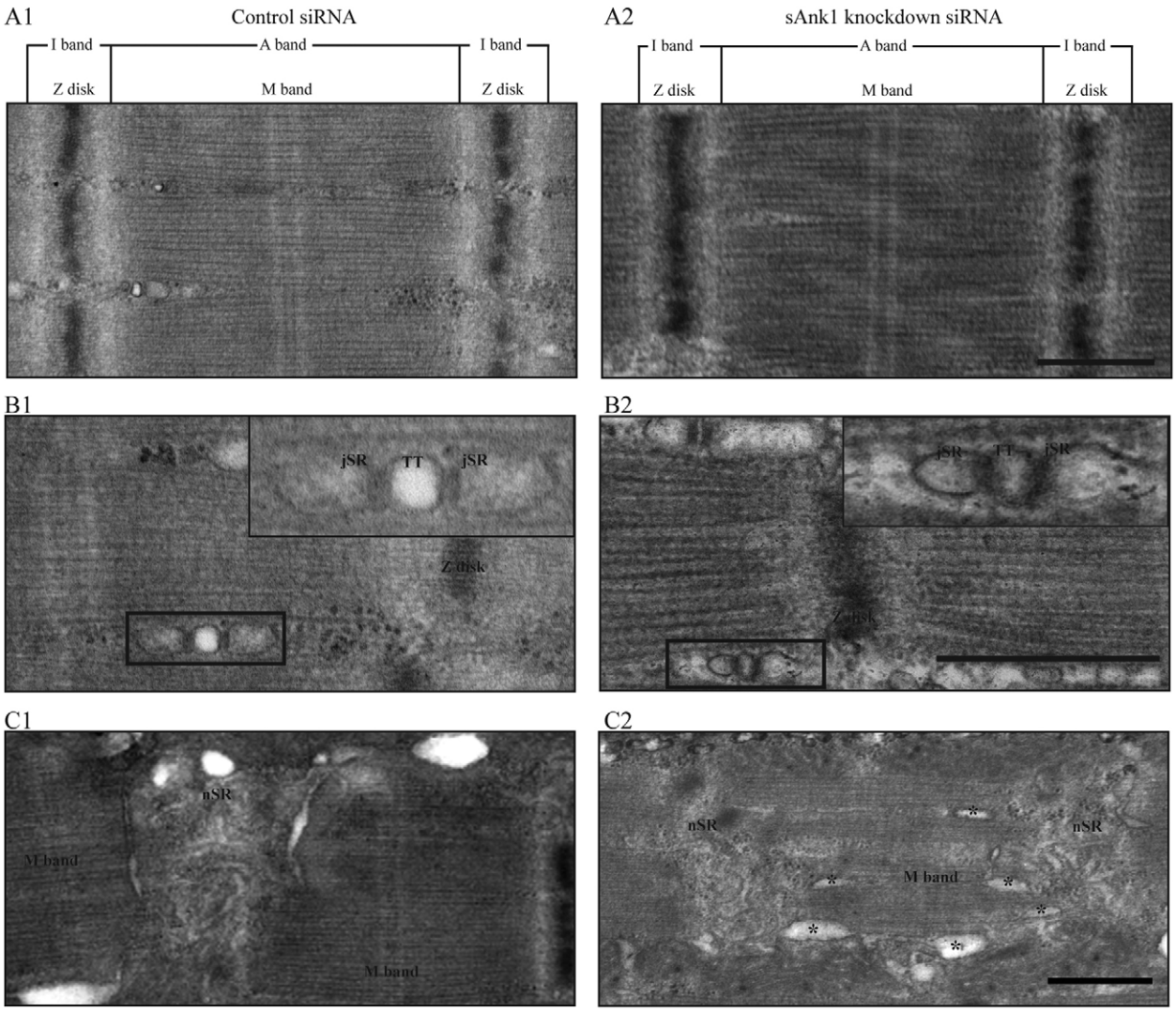

Fig. 7. Ultrastructure of fibers with reduced levels of sAnk1. FDB myofibers were treated as above, then fixed and processed for thin-section electron microscopy. Views are of the sarcomere (**A**), triad junctions (**B**) (comprised of t-tubules flanked on either side by jSR) and nSR (**C**). Sections through a myofiber treated with con-siRNA show typical structures (A1,B1,C1). Fibers treated with sAnk1-siRNA have sarcomeres and triad junctions that appear normal, as in controls (A2,B2,C2). However, the nSR does not appear as an extensive system of anastomosing tubules overlying the Z-disk, as it does in controls. Instead, it appears reduced in size and complexity, with prominent and enlarged tubular elements organized parallel to the long axis of the fiber (asterisks). Scale bar: 0.5 μm.

expression with siRNA. We report that sAnk1-siRNA reduces the expression of sAnk1 and selectively destabilizes the nSR, with no apparent effects on the contractile apparatus and relatively minor effects on the organization of the jSR. In severely affected myofibers, the remnants of the nSR form at least two distinct structures, one rich in sAnk1 and SLN, the other rich in SERCA. The amount of Ca^{2+} released from the SR and the rate of reuptake of Ca^{2+} are both significantly altered in sAnk1-siRNA-treated myofibers, which is consistent with the loss of the nSR. Our results suggest that the integral membrane proteins of the nSR segregate when that compartment is disrupted. They further indicate that the integrity of the jSR does not depend on that of the nSR, whereas the integrity of the nSR requires sAnk1.

We used an siRNA targeted to the 5′ UTR of sAnk1, identified in a BLAST search as unique to muscle-specific small ankyrins, to reduce its expression. Selecting a sequence to target sAnk1 specifically, without affecting the expression of other forms of ankyrins present in muscle, is challenging, primarily because the short coding sequence of sAnk1 shares homology with several other ankyrins. Our targeting sequence, located in the unique 5′ UTR, effectively reduced the amount of sAnk1 mRNA and protein in skeletal myofibers by approximately twofold, while having no measurable effect on the other forms of ankyrins we assayed.

Remarkably, two other proteins of the nSR, SERCA and SLN, decreased in amount when sAnk1 expression was reduced. Their loss occurs after transcription and mRNA processing, because the amount of their corresponding mRNAs was not affected by knockdown of sAnk1. The most likely explanation for these results is that the nSR becomes destabilized when sAnk1 is reduced, and that in the absence of this compartment both SERCA and SLN are unstable and, therefore, degraded. The effect on SERCA is specifically caused by the reduced levels of

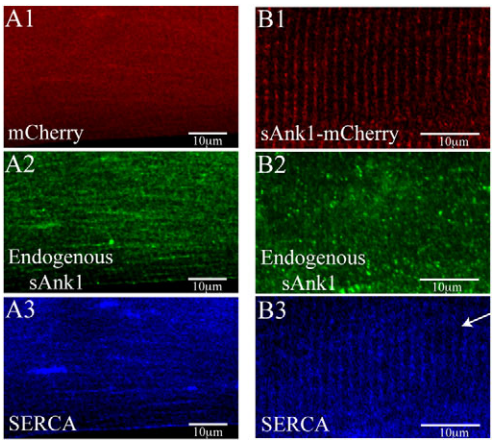

Fig. 8. sAnk1–mCherry restores SR structure lost by knockdown of endogenous sAnk1. FDB fibers were transfected in vivo by electroporation, either with a plasmid encoding mCherry (**A**) or mCherry–sAnk1 (**B**). One week later, fibers were cultured, treated with sAnk1-siRNA and labeled for immunofluorescence of sAnk1 and SERCA. The results show that, although the knockdown of expression of endogenous sAnk1 in these fibers was considerable and resulted in significant disorganization of the remaining sAnk1 (A2 and B2), the striated organization of SERCA in the nSR is specifically rescued by sAnk1-mCherry (B3) but not by mCherry alone (A3). Scale bar: 10 μm. Arrow indicates Z-disk.

sAnk1, because restoring sAnk1 to myofibers as an mCherry fusion protein preserved the localization of SERCA around Z-disks.

It is not yet known whether knockdown of SERCA or SLN can have a similar effect on sAnk1 expression or organization. Knockdown of SERCA or SLN has no noticeable effect on other Ca^{2+} handling proteins, however (Babu et al., 2007; Pan et al., 2003). Our results are consistent with the idea that sAnk1 interacts directly with either SERCA or SLN. Both sAnk1 and SLN are small, integral membrane proteins with distinctive, single-pass transmembrane domains that, similarly to the transmembrane sequences of phospholamban and glycophorin (Fujii et al., 1989; Lemmon et al., 1992; Simmerman et al., 1996), might mediate the formation of homo- or hetero-oligomers that participate in the assembly or stabilization of the nSR.

Although the most prominent effect of inhibiting sAnk1 synthesis is on the nSR, myofibers with reduced sAnk1 also show minor, albeit significant, alterations in other compartments of the SR. In myofibers showing moderate losses of sAnk1, the longitudinal elements of the SR can become more prominent and accumulate some proteins more typical of the jSR, such as calsequestrin. By contrast, in myofibers showing more severe losses of sAnk1, the organization of the jSR and the proteins that comprise it are retained, suggesting that the small changes we observed in the jSR are likely to be secondary to the primary effects of sAnk1 knockdown on the proteins of the nSR. Our ultrastructural observations, which have so far been limited to cells that appear to be only moderately affected by sAnk1-siRNA, are qualitatively consistent with this conclusion.

Our results show that SLN, but not SERCA, colocalizes with sAnk1 in myofibers in which sAnk1 levels are severely reduced. It is unclear whether the compartments containing these proteins are tubular or vesicular in structure, but we speculate that they are

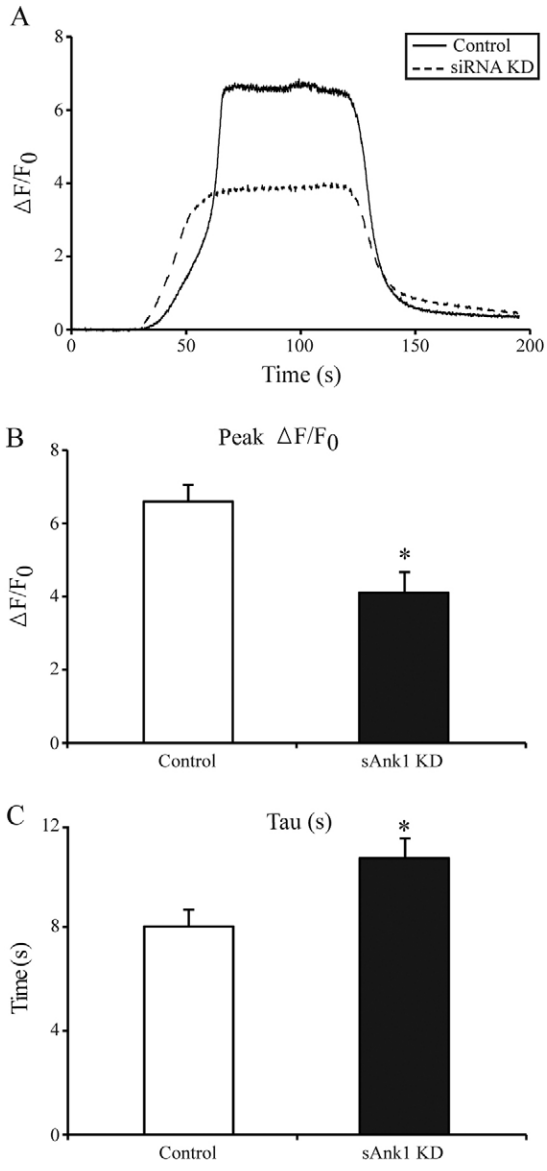

Fig. 9. Ca^{2+} transients in fibers with reduced levels of sAnk1. FDB fibers treated as in Fig. 1 were loaded with Fluo-4 to measure the $[Ca^{2+}]_i$ transient induced by exposure to the RyR1 agonist, 4-CmC (1 mM). (**A**) Representative fluorescence profiles are of confocal line-scan images from con-siRNA-treated (solid line) and sAnk1-siRNA-treated (dashed line) myofibers. The latter shows lower peak fluorescence. (**B**) Data from three experiments, performed as in A were pooled. The peak of the $[Ca^{2+}]_i$ transient in fibers treated with sAnk1-siRNA is significantly smaller than controls ($*P<0.01$). (**C**) Following washout of 4-CmC, the rapid decay phase of the $[Ca^{2+}]_i$ transient was fitted by a single-exponential to determine tau. Tau of the $[Ca^{2+}]_i$ transient is significantly slower in sAnk1-siRNA-treated myofibers than in controls ($*P<0.01$). The data show that the size and rate of refilling of Ca^{2+} stores in FDB myofibers are reduced when sAnk1 expression is inhibited by siRNA. Results are means ± s.e.m.

involved in formation as well as breakdown of the nSR compartment. The fact that sAnk1 is among the earliest of SR proteins to concentrate around Z-disks as muscle cells develop (Giacomello and Sorrentino, 2009) is congruent with our data and with the idea that it plays a morphogenetic role in assembling and stabilizing the nSR.

Our studies with Fluo-4 indicate that sAnk1-siRNA-treated myofibers release less Ca^{2+} from SR stores and refill those stores more slowly than controls. Both results are consistent with the measured decrease in SERCA, secondary to the knockdown of sAnk1. Although the magnitude of these effects is somewhat smaller than might be predicted from the ~2-fold decrease in the amount of SERCA we observed, they can be explained by our observation that the residual SERCA fails to associate with SLN, which would enhance SERCA pumping (Babu et al., 2007) and partially dampen the effect of lower SERCA expression. Although changes in $[Ca^{2+}]_{SR}$ do not alter the ability of the SR to release Ca^{2+} when stimulated, decreasing SR Ca^{2+} uptake might have significant effects on EC coupling and cell survival. We speculate that differences in Ca^{2+} regulation in sAnk1-siRNA-treated myofibers increases cytosolic $[Ca^{2+}]$, altering contractile activity, signaling pathways and proteolysis, leading to small changes in the organization of the jSR. However, we cannot rule out the possibility that small amounts of sAnk1 normally reside in the jSR and that knockdown has direct, albeit minor, effects on its organization.

Our studies show that downregulation of sAnk1 results in the disruption of the nSR and the destabilization of two of the proteins typically found in this membrane compartment. Thus, our findings offer the first evidence that sAnk1 is necessary for the stability of the nSR. Ank1 is required for the stability of the plasma membrane of the mammalian erythrocyte (White et al., 1990), but to our knowledge this is the first example of an ankyrin protein being required for the structural and functional integrity of an intracellular membrane. Although sAnk1 might also function in muscle to organize the SR through its interactions with obscurin (Bagnato et al., 2003; Kontrogianni-Konstantopoulos et al., 2003), our current results indicate that sAnk1 has a much broader role in the morphogenesis and stability of the SR.

Materials and Methods

Animals

All animals were used in accordance to protocols approved by the Institutional Animal Care and Use Committee of the University of Maryland School of Medicine and in accordance with NIH guidelines.

Cultures of Skeletal Myofibers

Primary cultures of muscle fibers were prepared from the flexor digitorum brevis (FDB) muscles of adult rats as previous described (Liu et al., 1997), with minor modifications. For the experiments of Fig. 8, FDB muscle was injected with 10 μg cDNA encoding sAnk1-mCherry (see below), and then electroporated as described (DiFranco et al., 2006). Cultures were transduced with adenoviral constructs 24 hours after initial plating and analyzed 48 hours after transfection.

siRNA adenoviral constructs and infection of adult primary cultures

siRNA constructs were designed on Tuschl's principles to inhibit the expression of murine sAnk1 (accession number: BC061219; Elbashir et al., 2001a; Elbashir et al., 2001b; Elbashir et al., 2001c). The sequence of rat sAnk1 is unpublished; however, at the protein level the mouse and rat homologues differ only by one amino acid. The siRNA target site selected is located ~150 nucleotides upstream of the start codon in the 5′ UTR and specific for the muscle-specific small isoforms of the *Ank1* gene (sAnk1/1.5, 1.6 and 1.9; as discussed above and shown in supplementary material Fig. S1), 5′-AATAAACAGGAGATAAAGAGA-3′, and control sequence, 5′-ACTACCGTTGTTATAGGTG-3′ (Ambion, Austin, TX). We prepared these sequences as oligonucleotides and cloned them directionally, using *Xho*I and *Hpa*I restriction sites, into a modified adenovirus bi-cistronic shuttle vector (pShuttle, Strategene, La Jolla, CA) derived by inserting a 1.9 kb fragment from pLL3.7 (Rubinson et al., 2003), containing the U6 promoter, *Xho*I and *Hpa*I cloning sites and encoding downstream EGFP driven by a CMV promoter. The authenticity of the constructs was verified by sequence analysis. In transduced FDB myofibers showing a loss of sAnk1, we could not detect GFP either at the protein or mRNA level (data not shown) and therefore it was not used as a reporter protein in these studies. sAnk1 and control siRNA adenoviruses were produced by the Virus Core (University of Maryland, Baltimore, MD).

Cultures of rat myofibers were transduced with 10^9 viral particles per ml of virus, encoding sAnk1-siRNA or a con-siRNA, in 1 ml DMEM for 1 hour at 37℃. Transduced cells were supplemented with 1 ml of DMEM containing 0.2% BSA and 0.1% gentamicin. After 48 hours, cultures were rinsed with PBS and either collected for lysates or processed for immunofluorescence labeling.

Experiments were repeated ~ten times and at least 30 cells were analyzed from each group in each experiment. Immunoblotting and RT-PCR were repeated at least three times from three different experiments and representative images are shown for each.

sAnk1–mCherry construct

We used PCR to construct a chimeric version of sAnk1 linked to mCherry at its C-terminus in the pmCherri-N1 vector (Clontech Laboratories). When transfected into COS cells, the chimeric protein encoded by this cDNA construct concentrated in the ER, but did not label with our sAnk1 antibody, presumably because the mCherry moiety blocked access of the antibodies to the epitope, located in the C-terminal 15 amino acids of sAnk1 (unpublished results). Similarly, the antibodies failed to label the fusion protein in immunoblots (unpublished results).

Antibodies

Primary antibodies included rabbit antibodies against sAnk1 (3 μg/ml) (Zhou et al., 1997), the C-terminal region of obscurin A ('obscurinC', 3 μg/ml) (Kontrogianni-Konstantopoulos et al., 2003), ankyrin G (1:1000; a generous gift from Peter J. Mohler, University of Iowa School of Medicine, Iowa City, IO) and to the two N-terminal Ig domains of titin ('titinZ', 3 μg/ml) (Kontrogianni-Konstantopoulos et al., 2006a). We also used mouse antibodies against α-actinin (1:400; Sigma), calsequestrin (1:1000) (Affinity Bioreagents, Golden, CO), DHPR (1:80; supernatant fraction, Developmental Studies Hybridoma Bank, Iowa City, IA), myomesin (1:15; supernatant fraction, Developmental Studies Hybridoma Bank), myosin (1:400; Sigma), ankyrinB (1:1000, a generous gift from P. Mohler), the two N-terminal Ig domains of obscurin ('obscurinN', 3 μg/ml) (Kontrogianni-Konstantopoulos et al., 2006b), RyR (1:400; Affinity Bioreagents) and SERCA (1:400; Affinity Bioreagents). In addition, we used a guinea pig antibody against the obscurin RhoGEF domain (obscurinRhoGEF, 3 μg/ml) (Bowman et al., 2008) and a goat antibody against SLN (1:50; Santa Cruz Biotechnology, Santa Cruz, CA). The SLN antibody was only used for immunofluorescence studies, because it was ineffective in immunoblotting, even when concentrated. Secondary antibodies were goat anti-mouse, goat anti-rabbit, goat anti-guinea pig and donkey anti-goat IgGs conjugated to Alexa Fluor 488, Alexa Fluor 568 or Cy5 for immunofluorescence (Molecular Probes, Eugene, OR; 1:200) or to alkaline phosphatase for immunoblotting (Jackson ImmunoResearch, West Grove, PA; 1:5000).

Immunofluorescence staining and confocal microscopy

Cultures were fixed with 2% paraformaldehyde for 15 minutes at room temperature, permeabilized with 0.1% Triton X-100 for 20 minutes at room temperature, and immunolabeled sequentially with primary and secondary antibodies, for 16 hours and 90 minutes, respectively as described (Kontrogianni-Konstantopoulos et al., 2003). Coverslips were mounted in Aqua-polymount (Polysciences, Warrington, PA), to reduce photobleaching and analyzed with a Zeiss 510 confocal microscope (Carl Zeiss, Tarrytown, NY) equipped with a 63×, numerical aperture 1.4 objective.

Fluorescence intensities and the organization of select markers were analyzed with ImageJ (version 1.41, NIH, Bethesda, MD) and Excel (Microsoft, Bellevue, WA). Intensities were calculated by averaging the mean pixel intensity of the entire myofiber and are reported as a percentage fluorescence intensity of controls. Statistical significance was determined with the Student's *t*-test, with significance set at $P<0.01$, $n=30$. Structural disruption was quantified as described (Ackermann et al., 2009), with minor modifications. Colocalization of sAnk1 and SERCA, and sAnk1 and SLN, in con-siRNA- and sAnk1-siRNA-treated fibers was determined using Pearson's correlation coefficient. Percentage change in colocalization was calculated and statistical significance was determined using Student's *t*-test ($P<0.01$).

Immunoblotting

Control and transduced myofiber cultures were washed with ice-cold PBS and scraped with a rubber policeman. Cells were resuspended in 10 mM $NaPO_4$, 2 mM EDTA, 10 mM NaN_3, 120 mM NaCl and 1% Nonidet P-40, pH 7.4, supplemented with Complete protease inhibitors (Roche, Indianapolis, IN), and passed through a 21 gauge syringe ten times. The lysates were subjected to centrifugation at 14,000 ***g*** for 15 minutes at 4℃. Soluble protein was determined with a Bradford assay (Bio-Rad, Hercules, CA). Approximately 75 μg of protein from each sample were processed for immunoblotting as described (Kontrogianni-Konstantopoulos et al., 2004); primary antibodies were used at 200 ng/ml. We used ImageJ software to quantify the average intensities of the immunoreactive bands from at least three

independent experiments and report the differences between experimental and control samples as percentage change.

Reverse transcription polymerase chain reaction (RT-PCR)

Total RNA was isolated with Trizol reagent (Invitrogen) and ~5 μg of RNA were reverse transcribed with the Superscript First Strand Synthesis System for RT-PCR (Invitrogen), following the manufacturer's instructions. The rat gene encoding sAnk1 was amplified with a set of primers specific for the coding region of sAnk1. In parallel experiments, cDNAs encoding sequences of SERCA, SLN, calsequestrin, obscurin, α-actinin, ankyrin 1.6 and ankyrin 1.9 were assessed. Oligonucleotides are listed in supplementary material Table S1. PCR products were analyzed by ethidium bromide staining following electrophoresis in 1% agarose gels, and their authenticity was verified by sequencing.

Electron microscopy

Primary cultures of cultured FDB fibers treated with con-siRNA and sAnk1-siRNA were fixed overnight in 2% glutaraldehyde, 5 mg/ml tannic acid in 0.2 M cacodylate buffer, pH 7.2, and then stained further with uranyl acetate, embedded and processed for thin-section electron microscopy, as described (Lovering et al., 2011), with the exception that, after embedding, myofibers were separated from the glass coverslips with hydrofluoric acid (Pumplin et al., 1993). Myofibers were sampled randomly and representative images are shown.

Imaging of SR $[Ca^{2+}]_i$ content

Primary cultures of FDB fibers, transduced with control virus or virus encoding sAnk1-siRNA, were incubated in the presence of Fluo-4 AM (10 μM), BAPTA-AM (10 μM) and N-benzyl-p-toluene sulfonamide (BTS; 25 μM; Sigma) in MEM medium (Invitrogen) containing 0.2% pluronic acid F127 and 1.5% DMSO (Invitrogen) for 30 minutes at room temperature. Following dye loading, the fibers were washed with a continuous flow of physiological saline solution (PSS), containing 140 mM NaCl, 0.5 mM $MgCl_2$, 0.3 mM NaH_2PO_4, 5 mM HEPES, 5.5 mM glucose, 1.8 mM $CaCl_2$, 5 mM KCl, pH 7.4.

$[Ca^{2+}]_i$ transients were recorded on an inverted confocal microscope (Axiovert 200M LSM-510; Zeiss) equipped with an oil-immersion objective (40×, 1.2 NA). Excitation used a 488 nm excitation laser, and emission was recorded through a 505 nm long pass filter with the microscope set in line-scan mode. Lines were recorded every 50 msecond, with a pinhole of 1.5 Airy units. Ca^{2+} release from the SR was induced by bath application of 1 mM 4-chloro-m-cresol (4-CmC) in PSS. When the fluorescence signal reached a plateau, the 4-CmC was washed out with PSS.

Images were analyzed first with ImageJ, to create fluorescence profiles of each line-scan image, and then with Excel and Prism 4.0 (Graphpad Software, La Jolla, CA). Raw fluorescence was converted to $\Delta F/F_0$ to normalize to the background fluorescence level of Fluo-4 in resting fibers. The peak of the 4-CmC-induced $[Ca^{2+}]_i$ transient and the decay constant, tau, were calculated from the resulting curves. Tau was determined by fitting a single exponential to the fast phase of the recovery of the transient. Experiments were repeated three times, yielding an n value of 14 and 17 in the con-siRNA and sAnk1-siRNA-treated groups, respectively.

Acknowledgements

We thank B.L. Prosser for helpful discussions and assistance with statistical analysis. We also thank P. Mohler, University of Iowa School of Medicine, Iowa City, IO for antibodies against ankyrin B and ankyrin G.

Funding

Our research has been supported by grants from the National Institutes of Health [F32 AR52768 to M.A.A.; F32 AR057647 to A.P.Z.; RO1 AR52768, to A.K.K.; RO1 HL64304 and RO1 AR56330 to R.J.B] and from the Muscular Dystrophy Association. Deposited in PMC for release after 12 months.

Supplementary material available online at
http://jcs.biologists.org/lookup/suppl/doi:10.1242/jcs.085159/-/DC1

References

Ackermann, M. A., Hu, L. Y., Bowman, A. L., Bloch, R. J., and Kontrogianni-Konstantopoulos, A. (2009). Obscurin interacts with a novel isoform of MyBP-C slow at the periphery of the sarcomeric M-band and regulates thick filament assembly. *Mol. Biol. Cell* **20**, 2963-2978.

Babu, G. J., Bhupathy, P., Timofeyev, V., Petrashevskaya, N. N., Reiser, P. J., Chiamvimonvat, N., and Periasamy, M. (2007). Ablation of sarcolipin enhances sarcoplasmic reticulum calcium transport and atrial contractility. *Proc. Natl. Acad. Sci. USA* **104**, 17867-17872.

Bagnato, P., Barone, V., Giacomello, E., Rossi, D., and Sorrentino, V. (2003). Binding of an ankyrin-1 isoform to obscurin suggests a molecular link between the sarcoplasmic reticulum and myofibrils in striated muscles. *J. Cell Biol.* **160**, 245-253.

Birkenmeier, C. S., Sharp, J. J., Gifford, E. J., Deveau, S. A., and Barker, J. E. (1998). An alternative first exon in the distal end of the erythroid ankyrin gene leads to production of a small isoform containing an NH2-terminal membrane anchor. *Genomics* **50**, 79-88.

Borzok, M. A., Catino, D. H., Nicholson, J. D., Kontrogianni-Konstantopoulos, A., and Bloch, R. J. (2007). Mapping the binding site on small ankyrin 1 for obscurin. *J. Biol. Chem.* **282**, 32384-32396.

Bowman, A. L., Catino, D. H., Strong, J. C., Randall, W. R., Kontrogianni-Konstantopoulos, A., and Bloch, R. J. (2008). The rho-guanine nucleotide exchange factor domain of obscurin regulates assembly of titin at the Z-disk through interactions with Ran binding protein 9. *Mol. Biol. Cell* **19**, 3782-3792.

DiFranco, M., Neco, P., Capote, J., Meera, P., and Vergara, J. L. (2006). Quantitative evaluation of mammalian skeletal muscle as a heterologous protein expression system. *Protein Expr. Purif.* **47**, 281-288.

Elbashir, S. M., Harborth, J., Lendeckel, W., Yalcin, A., Weber, K., and Tuschl, T. (2001a). Duplexes of 21-nucleotide RNAs mediate RNA interference in cultured mammalian cells. *Nature* **411**, 494-498.

Elbashir, S. M., Lendeckel, W., and Tuschl, T. (2001b). RNA interference is mediated by 21- and 22-nucleotide RNAs. *Genes. Dev.* **15**, 188-200.

Elbashir, S. M., Martinez, J., Patkaniowska, A., Lendeckel, W., and Tuschl, T. (2001c). Functional anatomy of siRNAs for mediating efficient RNAi in Drosophila melanogaster embryo lysate. *EMBO J.* **20**, 6877-6888.

Franzini-Armstrong, C., Ferguson, D. G., Castellani, L., and Kenney, L. (1986). The density and disposition of Ca-ATPase in in situ and isolated sarcoplasmic reticulum. *Ann. N. Y. Acad. Sci.* **483**, 44-56.

Franzini-Armstrong, C., Protasi, F., and Tijskens, P. (2005). The assembly of calcium release units in cardiac muscle. *Ann. N. Y. Acad. Sci.* **1047**, 76-85.

Fujii, J., Maruyama, K., Tada, M., and MacLennan, D. H. (1989). Expression and site-specific mutagenesis of phospholamban. Studies of residues involved in phosphorylation and pentamer formation. *J. Biol. Chem.* **264**, 12950-12955.

Giacomello, E., and Sorrentino, V. (2009). Localization of ank1.5 in the sarcoplasmic reticulum precedes that of SERCA and RyR: relationship with the organization of obscurin in developing sarcomeres. *Histochem. Cell Biol.* **131**, 371-382.

Gyorke, S., Gyorke, I., Terentyev, D., Viatchenko-Karpinski, S., and Williams, S. C. (2004). Modulation of sarcoplasmic reticulum calcium release by calsequestrin in cardiac myocytes. *Biol. Res.* **37**, 603-607.

Hopitzan, A. A., Baines, A. J., Ludosky, M. A., Recouvreur, M., and Kordeli, E. (2005). Ankyrin-G in skeletal muscle: tissue-specific alternative splicing contributes to the complexity of the sarcolemmal cytoskeleton. *Exp. Cell Res.* **309**, 86-98.

Jorgensen, A. O., Shen, A. C., MacLennan, D. H., and Tokuyasu, K. T. (1982). Ultrastructural localization of the Ca2+ + Mg2+-dependent ATPase of sarcoplasmic reticulum in rat skeletal muscle by immunoferritin labeling of ultrathin frozen sections. *J. Cell Biol.* **92**, 409-416.

Kontrogianni-Konstantopoulos, A., and Bloch, R. J. (2003). The hydrophilic domain of small ankyrin-1 interacts with the two N-terminal immunoglobulin domains of titin. *J. Biol. Chem.* **278**, 3985-3991.

Kontrogianni-Konstantopoulos, A., and Bloch, R. J. (2005). Obscurin: a multitasking muscle giant. *J. Muscle. Res. Cell Motil.* **26**, 419-426.

Kontrogianni-Konstantopoulos, A., Jones, E. M., Van Rossum, D. B., and Bloch, R. J. (2003). Obscurin is a ligand for small ankyrin 1 in skeletal muscle. *Mol. Biol. Cell.* **14**, 1138-1148.

Kontrogianni-Konstantopoulos, A., Catino, D. H., Strong, J. C., Randall, W. R., and Bloch, R. J. (2004). Obscurin regulates the organization of myosin into A bands. *Am. J. Physiol. Cell Physiol.* **287**, C209-C217.

Kontrogianni-Konstantopoulos, A., Catino, D. H., Strong, J. C., and Bloch, R. J. (2006a). De novo myofibrillogenesis in C2C12 cells: evidence for the independent assembly of M bands and Z disks. *Am. J. Physiol. Cell Physiol.* **290**, C626-C637.

Kontrogianni-Konstantopoulos, A., Catino, D. H., Strong, J. C., Sutter, S., Borisov, A. B., Pumplin, D. W., Russell, M. W., and Bloch, R. J. (2006b). Obscurin modulates the assembly and organization of sarcomeres and the sarcoplasmic reticulum. *FASEB J.* **20**, 2102-2111.

Kontrogianni-Konstantopoulos, A., Ackermann, M. A., Bowman, A. L., Yap, S. V., and Bloch, R. J. (2009). Muscle giants: molecular scaffolds in sarcomerogenesis. *Physiol. Rev.* **89**, 1217-1267.

Kordeli, E., Ludosky, M. A., Deprette, C., Frappier, T., and Cartaud, J. (1998). AnkyrinG is associated with the postsynaptic membrane and the sarcoplasmic reticulum in the skeletal muscle fiber. *J. Cell Sci.* **111 (Pt 15)**, 2197-2207.

Lange, S., Ouyang, K., Meyer, G., Cui, L., Cheng, H., Lieber, R. L., and Chen, J. (2009). Obscurin determines the architecture of the longitudinal sarcoplasmic reticulum. *J. Cell Sci.* **122**, 2640-2650.

Lemmon, M. A., Flanagan, J. M., Hunt, J. F., Adair, B. D., Bormann, B. J., Dempsey, C. E., and Engelman, D. M. (1992). Glycophorin A dimerization is driven by specific interactions between transmembrane alpha-helices. *J. Biol. Chem.* **267**, 7683-7689.

Liu, Y., Carroll, S. L., Klein, M. G., and Schneider, M. F. (1997). Calcium transients and calcium homeostasis in adult mouse fast-twitch skeletal muscle fibers in culture. *Am. J. Physiol.* **272**, C1919-C1927.

Lovering, R. M., O'Neill, A., Muriel, J. M., Prosser, B. L., Strong, J., and Bloch R. J. (2011) Physiology, structure, and susceptibility to injury of skeletal muscle in mice lacking keratin 19-based and desmin-based intermediate filaments. *Am. J. Physiol. Cell Physiol.* **300**, C803-C813.

Mohler, P. J. (2006). Ankyrins and human disease: what the electrophysiologist should know. *J. Cardiovasc. Electrophysiol.* **17**, 1153-1159.

Odermatt, A., Becker, S., Khanna, V. K., Kurzydlowski, K., Leisner, E., Pette, D., and MacLennan, D. H. (1998). Sarcolipin regulates the activity of SERCA1, the fast-twitch skeletal muscle sarcoplasmic reticulum Ca2+-ATPase. *J. Biol. Chem.* **273**, 12360-12369.

Pan, Y., Zvaritch, E., Tupling, A. R., Rice, W. J., de Leon, S., Rudnicki, M., McKerlie, C., Banwell, B. L., and MacLennan, D. H. (2003). Targeted disruption of the ATP2A1 gene encoding the sarco(endo)plasmic reticulum Ca2+ ATPase isoform 1 (SERCA1) impairs diaphragm function and is lethal in neonatal mice. *J. Biol. Chem.* **278**, 13367-13375.

Porter, N. C., Resneck, W. G., O'Neill, A., Van Rossum, D. B., Stone, M. R., and Bloch, R. J. (2005). Association of small ankyrin 1 with the sarcoplasmic reticulum. *Mol. Membr. Biol.* **22**, 421-432.

Rubinson, D. A., Dillon, C. P., Kwiatkowski, A. V., Sievers, C., Yang, L., Kopinja, J., Rooney, D. L., Zhang, M., Ihrig, M. M., McManus, M. T., et al. (2003). A lentivirus-based system to functionally silence genes in primary mammalian cells, stem cells and transgenic mice by RNA interference. *Nat. Genet.* **33**, 401-406.

Samuelsson, S. J., Luther, P. W., Pumplin, D. W., and Bloch, R. J. (1993). Structures linking microfilament bundles to the membrane at focal contacts. *J. Cell Biol.* **122**, 485-496.

Schneider, M. F., and Chandler, W. K. (1973). Voltage dependent charge movement of skeletal muscle: a possible step in excitation-contraction coupling. *Nature* **242**, 244-246.

Simmerman, H. K., Kobayashi, Y. M., Autry, J. M., and Jones, L. R. (1996). A leucine zipper stabilizes the pentameric membrane domain of phospholamban and forms a coiled-coil pore structure. *J. Biol. Chem.* **271**, 5941-5946.

White, R. A., Birkenmeier, C. S., Lux, S. E., and Barker, J. E. (1990). Ankyrin and the hemolytic anemia mutation, nb, map to mouse chromosome 8: presence of the nb allele is associated with a truncated erythrocyte ankyrin. *Proc. Natl. Acad. Sci. USA* **87**, 3117-3121.

Zhou, D., Birkenmeier, C. S., Williams, M. W., Sharp, J. J., Barker, J. E., and Bloch, R. J. (1997). Small, membrane-bound, alternatively spliced forms of ankyrin 1 associated with the sarcoplasmic reticulum of mammalian skeletal muscle. *J. Cell Biol.* **136**, 621-631.